



## Supporting Information

for

### Controllable physicochemical properties of $\text{WO}_x$ thin films grown under glancing angle

Rupam Mandal, Aparajita Mandal, Alapan Dutta, Rengasamy Sivakumar,  
Sanjeev Kumar Srivastava and Tapobrata Som

*Beilstein J. Nanotechnol.* **2024**, *15*, 350–359. doi:10.3762/bjnano.15.31

## Supplementary data

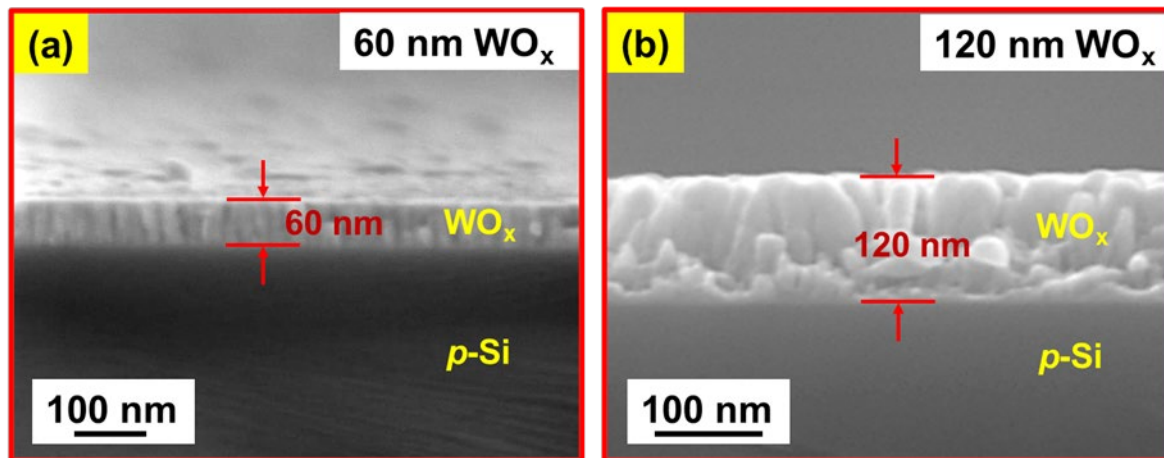


**Figure S1:** (a, b) XSEM images of 60 and 120 nm thick  $\text{WO}_x$  thin films deposited on p-Si substrates.

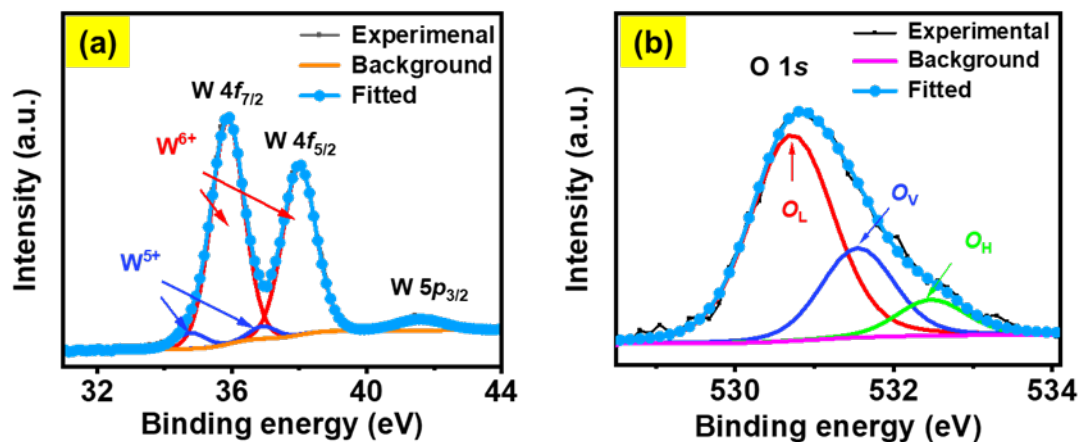


**Figure S2:** (a, b) XPS W 4f and O 1s core level spectra of as-deposited  $\text{WO}_x$  films having a thickness of 30 nm.

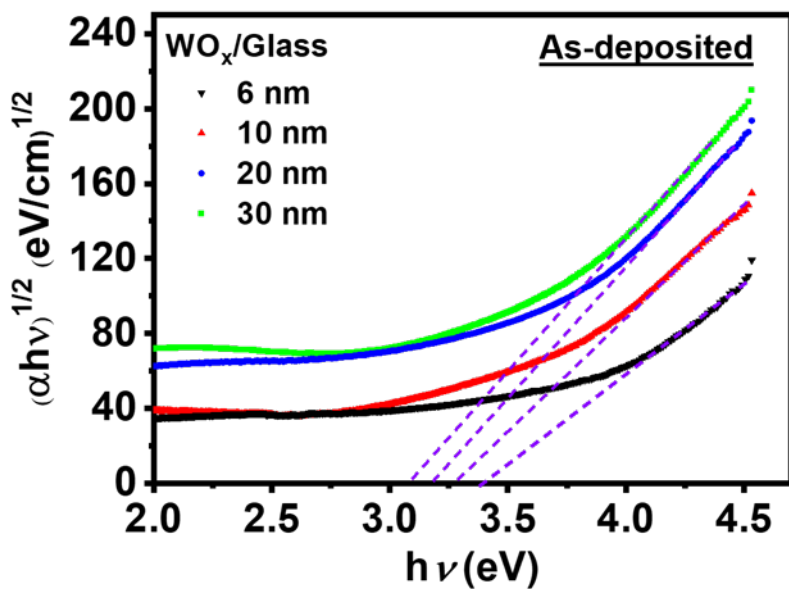


**Figure S3:** Tauc plots of the as-deposited nanostructured  $\text{WO}_x$  for different film thicknesses. The dashed lines indicate the intercept of the extrapolates on the  $x$  axis, providing the corresponding bandgap energies.

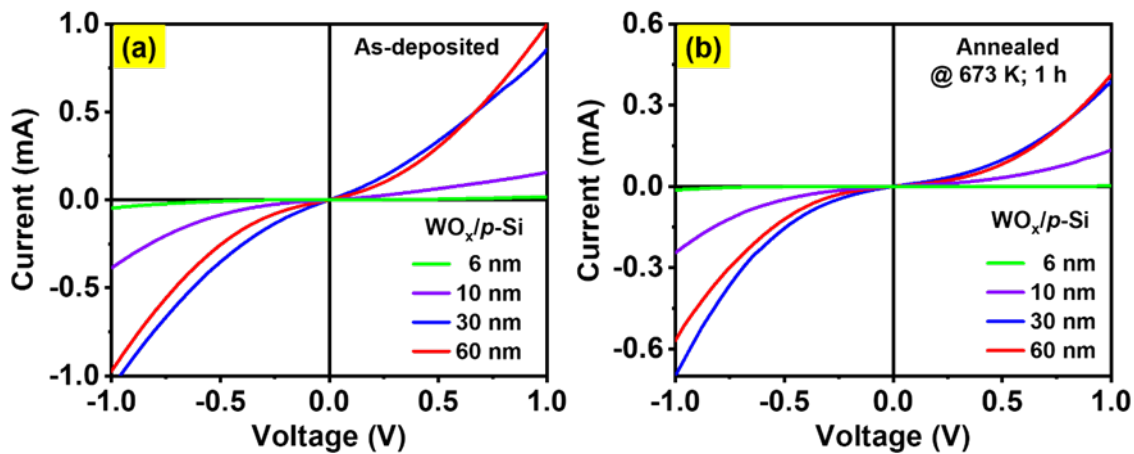


**Figure S4:** Linear  $I-V$  curves of (a) as-deposited and (b) annealed  $\text{WO}_x/\text{p-Si}$  heterostructures for different  $\text{WO}_x$  film thicknesses.

**Table S1:** Comparison between the present work and previously reported works on nanostructured WO<sub>3</sub> films.

Film thickness (nm)	Growth technique	Target used	Growth geometry	Optical studies	Electrical studies	Local probe studies	Post-growth annealing	Ref.
25–54	DC sputtering	W	GLAD	transmittance, bandgap, refractive index	<i>I</i> – <i>V</i>	NA	400 °C	[1]
500	reactive DC magnetron sputtering	W	GLAD	NA	current response for gas sensing	NA	400 and 500 °C	[2]
100	pulsed DC magnetron sputtering	W	GLAD	none (only structural and morphological studies)	NA	NA	500 °C	[3]
270, 500	e-beam evaporation	WO <sub>3</sub>	GLAD	transmittance	<i>I</i> – <i>V</i>	NA	100, 200, 300, 350, and 400 °C	[4]
1000	reactive DC magnetron sputtering	W	GLAD	transmittance, refractive index, bandgap	NA	NA	NA	[5]
300	reactive DC magnetron sputtering	W	GLAD	transmittance	NA	NA	NA	[6]
6–120 nm	RF magnetron sputtering	WO <sub>3</sub>	GLAD	transmittance, bandgap	<i>I</i> – <i>V</i>	Local work function	400 °C	present work

## References

1. Rydosz, R.; Dyndał, K.; Kollbe, K.; Andrysiewicz, W.; Sitarz, M.; Marszałek, K. *Vacuum* **2020**, *177*, 109378. doi:10.1016/j.vacuum.2020.109378
2. Horprathum, M.; Frankel, D. J.; Lad, R. J. *Sens. Actuators, B* **2013**, *176*, 685–691. doi:10.1016/j.snb.2012.09.077
3. Deniz, D.; Frankel, D. J.; Lad, R. J. *Thin Solid Films* **2010**, *518*, 4095–4099. doi:10.1016/j.tsf.2009.10.153
4. Yuan, J.; Wang, B.; Wang, H.; Chai, Y.; Jin, Y.; Qi, H.; Shao, H. *Appl. Surf. Sci.* **2018**, *447*, 471–478. doi:10.1016/j.apsusc.2018.03.248
5. Sakkas, C.; Rauch, J.-Y.; Cote, J.-M.; Tissot, V.; Gavoille, J.; Martin, N. *Coatings* **2021**, *11*, 438. doi:10.3390/coatings11040438
6. Salawan, C.; Aiempakanit, M.; Aiempakanit, K.; Chanonnonnawathorn, C.; Eiamchai, P.; Horprathum, M. *Mater. Today: Proc.* **2017**, *4*, 6423–6429. doi:10.1016/j.matpr.2017.06.148